Taylor & Francis
Taylor & Francis Group

Ferroelectricity and Polarons in $Sn_2P_2S_6$ Crystals

YU. VYSOCHANSKII,* A. MOLNAR, R. YEVYCH, K. GLUKHOV, AND M. MEDULYCH

Uzhgorod University, Uzhgorod 88000, Ukraine

For $Sn_2P_2S_6$ ferroelectric-semiconductor the relaxation processes at low temperatures in the ferroelectric phase were investigated by low frequency dielectric and Raman spectroscopies. Observed anomalies in dielectric losses and their change under illumination together with lattice anharmonicity appearance in Raman spectral bands shape are compared with previous data on photo- and thermoluminescence. The experimental data are analyzed with consideration of local three-well potential in ground state and explained by creation and annihilation of small hole and electron polarons with participation of tin vacancies acceptor and sulfur vacancies donor in gap energy states.

I. Introduction

$Sn_2P_2S_6$ (SPS) ferroelectric-semiconductor is photorefractive [1], photovoltaic [2], and piezoelectric [3] material. The proper ferroelectric second order phase transition at $T_0 \approx$ 337 K (P2$_1$/n $\rightarrow$ Pn) is related with displacive—order/disorder dynamics [4]. The lattice instability is determined by $A_g B_u^2$ nonlinear interaction of the fully symmetrical A_g and soft polar B_u optic modes [5]. The stereoactivity of tin cations $5s^2$ lone pair electrons was supposed as driven force of ferroelectricity. In results of electron spectra investigations [6] the origin of ferroelectricity in SPS has been described as sequence of several steps. The change of the electron density charge distribution in the elementary cell by fully symmetric breathing modes A_g assists as first step. This redistribution of the electron density prompts the stereochemical activity of tin cations electron lone pair and produces the covalence bonds of tin atoms with sulfur and phosphorous atoms, which could be considered as second part. At the third stage, the weakening of the short-range repulsion between cations of tin and phosphorus occurs, as a result of their charges lowering, at significant coulomb repulsion of the nearest tin cations. Mentioned second and third factors represent the nonlinear interaction of $A_g B_u^2$ type, they govern anisotropy of polar shifting of atoms and define appearance of the dipole structure motives, which are related to the polar normal coordinates of B_u symmetry. The fourth important factor is the dipole-dipole interaction, which correlates orientation of local dipoles and defines appearance of the spontaneous polarization in the crystal structure.

Semiconductor properties of SPS crystals are related to the sulfur vacancies deep donor states and to the tin vacancies shallow acceptor states in the energy gap [7, 8]. To

the scheme of the local states in the gap, the deep energy level of small electron polarons, which are selftrapped at Sn^+ cations, and shallow energy levels of small hole polarons that are trapped at S^- anions, were also added. Such energy scheme has been also successfully used [7] for explanation of observed phenomena of photoinduced optical absorption [9] and photoinduced EPR signals [10], and also for description of photorefractive and thermoelectric properties of SPS crystals [8]. Peculiarities of the local states, namely shallow energy position of acceptors together with levels of hole polarons, and deep energy levels of the donor centers, obviously are related to the ionic-covalence character of crystalline structure. There are a very highly charged anionic complexes $(P_2S_6)^{4-}$ (which are built by covalence P—S and P—P bonds). These anions are joined by Sn^{2+} cations. Certainly, the ionic charges are not unique because of some covalence of Sn—S bonds. Named in gap local states clearly determine the "p"-type dark conductivity of SPS crystals at room temperature and their inversion to "n"-type conductivity at heating above ≈450 K as follows from thermoelectric data [8].

For verification of considered picture of electrons trapping, the probing in different spectral ranges could be informative. The electronic transitions with participation of localized states could be checked by analysis of luminescence data. The Raman spectroscopy is an effective tool for characterization of the lattice anharmonicity. The low frequency dielectric investigations could present information concerning slow dynamics of polaronic particles [11]. In this paper possibility of polaronic exciton existence in the ferroelectric phase of SPS crystals is discussed by analysis of early founded photoluminescence (PL) temperature dependence [12, 13] and thermoluminescence data [14]. The dielectric susceptibility temperature anomalies across the ferroelectric phase are investigated for different frequencies in dark condition and under illumination. Several observed mechanisms of dielectric losses are related to relaxation of hole polarons with participation of the electron-hole compensation. The Raman scattering temperature dependence was investigated for characterization of the lattice anharmonicity in the ferroelectric phase that is related to the three-well shape of the local potential for the PT order parameter fluctuations. Also, influence of addition illumination on the Raman spectra has been studied. Comparison of photoluminescence temperature suppression with data about lattice anharmonicity presents evidence of join nature of ferroelectricity and polaronic states in SPS crystals.

II. Experimental Data

Dielectric susceptibility was investigated by Goodwill LCR-815 in frequency range $10-10^5$ Hz at temperature variation velocity 0.1 K/min. For the sample illumination the photodiode (LED TLCO5100 λ = 605 nm, I = 5000 mKd) was used. The vapor transport (VT) and Bridgeman (Br) technologies were used for the SPS single crystals growing. The investigated samples were prepared as plates with 5^*5^*3 mm^3 dimensions with silver paste electrodes on largest (001) face that was nearly normal to the spontaneous polarization direction. Raman scattering temperature dependence was investigated by double grating spectrometer with resolution near 1 cm^{-1} and at temperature stabilization better than 1 K. The He-Ne laser (6328 Å) was used for excitation of scattering in vapor transport grown SPS sample with dimensions 5^*5^*5 mm^3 at application of right-angle geometry Z(XX)Y with X and Y axes oriented along [100] and [010] crystallographic directions.

Earlier [15], the dielectric relaxation anomaly for the SPS crystals was found with dielectric losses maximum near 60 K at 10^4 Hz. The temperature-frequency behavior of this relaxation process is characterized by Arrhenius law with activation energy near
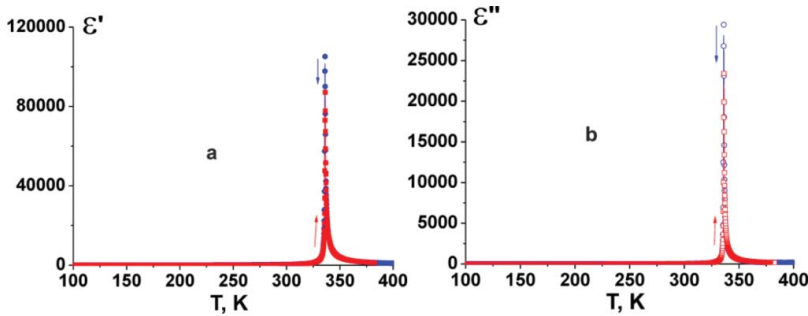
Figure 1. Temperature dependence of real (a) and imaginary parts (b) of dielectric susceptibility at 10^4 Hz in cooling and heating modes for Br SPS crystal.

0.1 eV and attempt frequency $3.5*10^{11}$ Hz. Also, losses peak was observed in 160–260 K temperature interval. The authors [15] have attributed the lowest temperature (near 60 K) relaxations to some disordering in the ferroelectric phase.

At T ≥ 250 K in the ferroelectric phase temperature behavior of dielectric suscepti-bility real and imaginary parts demonstrates clear temperature hysteresis and dependence on temperature variation velocity, and has high nonlinearity – dependence on measuring electric field amplitude. Here, the dielectric susceptibility could be effectively suppressed by the sample monodomenization by application of the strong ac electric field along polar direction. It was supposed [16] that the sample dependent strong nonerhodic dielectric contribution observed at T ≥ 250 K could be related to the domain walls.

Above mentioned data show that further investigations of the relaxation dielectric processes inside the ferroelectric phase of SPS crystals are needed and consideration of their relation to the possible polaronic contributions is actual.

The temperature dependences of dielectric susceptibility for the Br and VT SPS samples in the temperature range of 100–400 K are shown in Figs. 1 and 2. In addition to the strong anomaly near the second order PT at 337 K, for VT sample a peculiar relaxation behavior of susceptibility is observed in the paraelectric phase. Such relaxation anomaly is not observed for the Br SPS sample, but here the high dielectric losses are observed in the ferroelectric phase, just below the PT temperature.
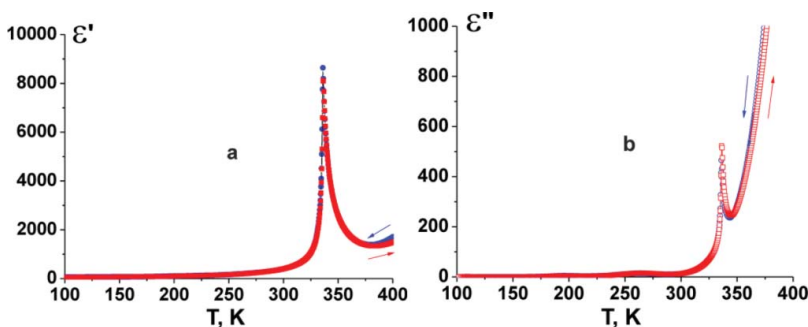
Figure 2. Temperature dependence of real (a) and imaginary (b) parts of dielectric susceptibility at 10^4 Hz in cooling and heating modes for VT SPS crystal.
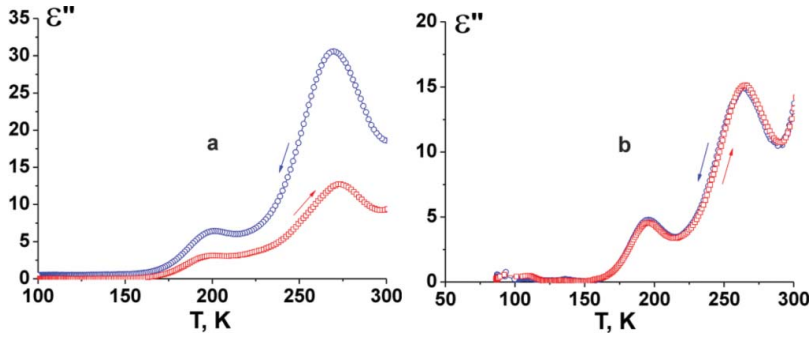
Figure 3. Low temperature range of temperature dependence at cooling and heating of dielectric losses at 10^4 Hz for Br (a) and VT (b) SPS crystals.

At lower temperatures two maxima of dielectric losses are observed similarly for both Br and VT samples (Fig. 3). These maxima are placed on background temperature tail of the domain walls dielectric contribution. This background tail demonstrates strong temperature hysteresis for Br crystal and it has not pronounced temperature hysteresis for VT sample.

The temperature dependences of dielectric losses for different frequencies (Fig. 4) clearly demonstrate relaxation behavior. The temperature evolution of related Cole-Cole diagrams could be fitted by Debye spectral relations with the smearing parameter α and Arrhenius behavior of relaxation time with $\tau_0^{-1} \approx 10^5$ Hz and 10^6 Hz and with activation energy $E_a \approx 0.23$ eV and 0.57 eV for the low and high temperature anomalies in the case of Br sample. Similar characteristics of dielectric relaxation processes were found for the VT SPS crystal. The smearing parameter is $\alpha \approx 0.5$ for both processes, which have losses maxima near 190 K and 270 K at 10^4 Hz (Figs. 3 and 4). It is important to note that similar
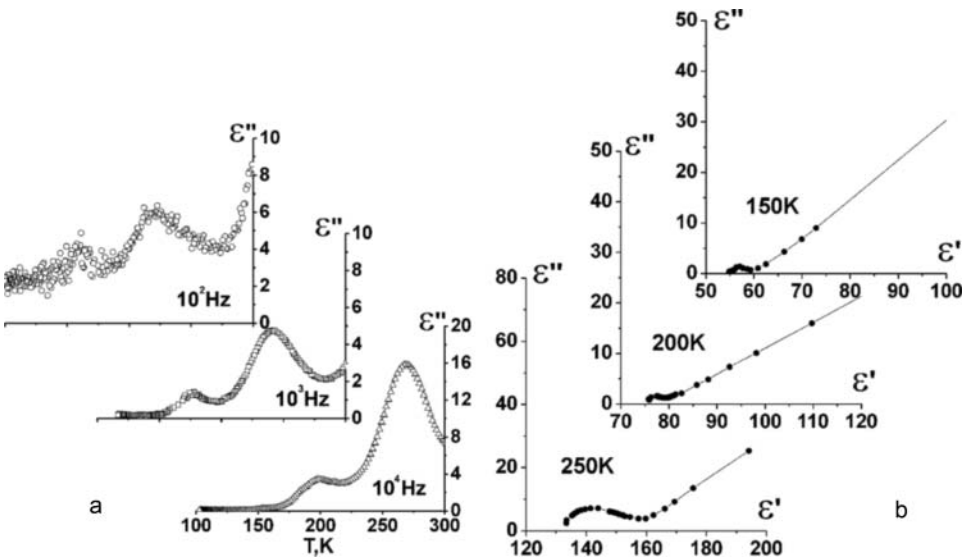
Figure 4. Low temperature range of dielectric losses temperature dependence at different frequencies (a) and Cole-Cole diagrams at different temperatures (b) for Br SPS crystal.
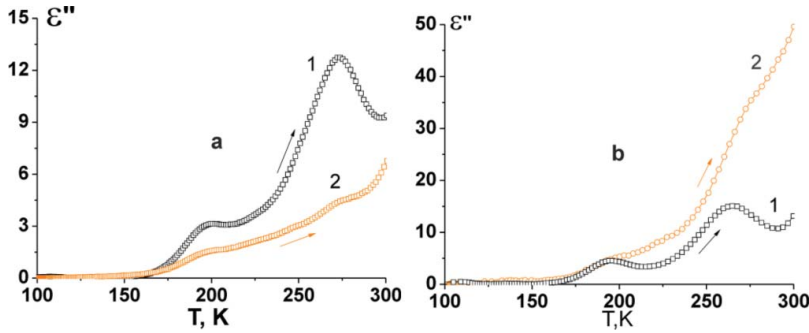
Figure 5. Low temperature range of temperature dependence at heating of dielectric losses at 10^4 Hz for Br (a) and VT (b) SPS crystals in dark conditions (1) and at illumination by orange light (2) (Figure available in color online).

value $\alpha \approx 0.5$ could be found at fitting of lower temperature (near 60 K) relaxation process on the data [15].

We also investigate the influence of illumination on the dielectric properties of SPS crystals (Fig. 5). For the Br sample illumination suppresses the low temperature anomalies of dielectric losses and elevates dielectric losses at high temperatures in the paraelectric phase. Opposite influence of lighting was observed for the VT SPS sample. Here, in the ferroelectric phase, at low temperatures, both losses maxima are improved by illumination and they are suppressed at high temperatures in the paraelectric phase.

The Raman spectra temperature dependence presents information about the crystal lattice anharmonicity. No equality of distances between energy levels of quantum anharmonic oscillator could be observed as splitting of additional (to the ones predicted by group theory) Raman spectral lines at temperature rising. For SPS crystal all low frequency external lattice vibrations and the highest frequency internal vibrations of P_2S_6 structure groups demonstrate rise of asymmetry of the Raman spectral lines and their smearing at heating, which is related to splitting of additional spectral bands. For example, the lowest frequency A' mode at 87 K is placed near 40 cm^{-1} and at heating additional bands deviation to lower frequencies occurs (Fig. 6). This deviation becomes clear at T $\geq$ 150 K that is connected with shape of the local anharmonic three-well potential (Fig. 7).

III. Analysis of Experimental Results

The Raman scattering data demonstrate strong lattice anharmonicity, which is related to electron-phonon interaction. Strongly anharmonic systems with different shapes of local potential have been theoretically analyzed in paper [17], and similar to experimentally observed (Figs. 6 and 7) temperature evolution of the phonon spectra with appearing of addition spectral lines was found. Some increase of the spectral intensity at the lowest frequencies appears (Fig. 6) at the SPS sample addition illumination during the Raman spectra recording. This fact obviously presents evidence about anharmonicity growing at electrons excitation across the energy gap.

Now we will show that the low temperature relaxation dielectric anomalies in SPS crystals obviously are related to the polarons motions in measuring electric field. Such supposal is based on comparison of characteristic frequencies and activation energies that follows from temperature dependences of dielectric and optic data, and agrees with scheme
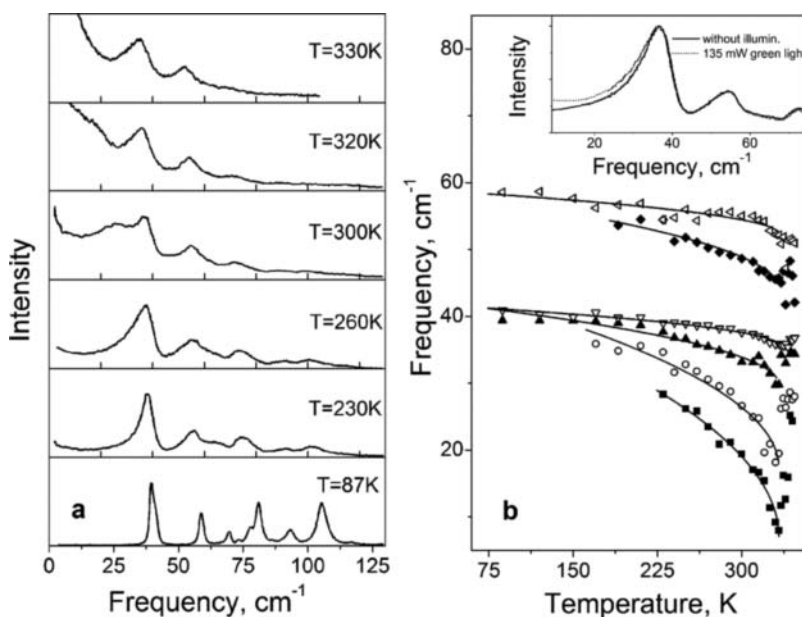
Figure 6. Temperature dependence of Raman scattering spectra (a) and low energy spectral bands frequencies (b) for VT SPS crystal. Insert at right—comparison of Raman spectra recording in usual condition and at addition illumination by in gap light.

[7] of local energetic states of small hole and electronic polarons together with acceptor and donor levels in the energy gap of SPS crystals.

The investigations of temperature dependence of PL spectra [12, 13] show the presence of strong orange peak with position in the range between 1.3 eV and 2 eV for different samples (Fig. 8). For the samples with dominate tin vacancies (that are "brown" or "dark" samples [9], or type I samples, as were named in Ref. [12]), strong PL is observed with spectral maximum near 1.6 eV [12, 13]. For SPS samples with big concentration of sulfur vacancies ("yellow" samples [9], or type II [12]) the spectral maxima of PL is placed near
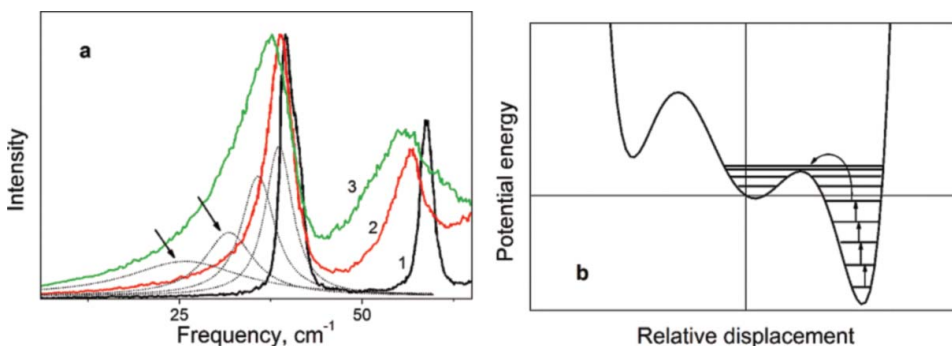
Figure 7. (a) The low frequency Raman spectra for VT SPS crystal at: 1 – 87 K, 2 – 210 K, 3 – 260 K. Specter at 260 K is fitted by Gaussian contours, the additional spectral lines are shown by arrows. (b) The local anharmonic potential.
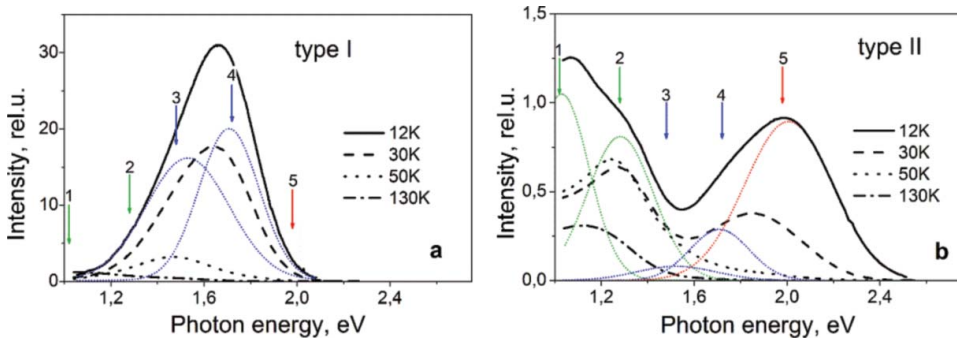
Figure 8. Photoluminescence spectra for VT SPS samples of type I (a) and type II (b) at different temperatures. The arrows show the maxima positions of Gaussian curves that fit experimental spectra [12].

2 eV and its intensity is weak by 30 times. At heating from 4.2 K till 130 K the intensity of strongest PL spectral lines, near 1.5 and 1.7 eV in the case of type I SPS sample, is strongly suppressed by activation manner with $E_a \approx 0.01$ eV (Fig. 9). Here, it should be noted that in PL for SPS crystals, generally five spectral lines were observed [12, 13] with the following numbering and energy positions: 1 – 1 eV; 2 – 1.3 eV; 3 – 1.5 eV; 4 – 1.7 eV; 5 – 2 eV. We propose next the explanation of these lines origin with account of the local energy state scheme (Fig. 10).

The "4" and "3" spectral lines are related to radiation annihilation of electron and hole polarons; the "2" and "1" lines are attributed to radiation recombination of the electron polarons with ionized donor centers; the "5" line belongs to radiation recombination of free electron from the conduction band with the ionized donor centers.

The most intensive PL spectral lines "3" and "4" obviously are related to annihilation of free polaronic excitons (Fig. 11a) S^- - Sn_1^+ and S^- - Sn_2^+, here Sn_1^+ and Sn_2^+ denote two types of tin cations in the ferroelectric phase, and S^- presents the sulfur ions (six types of sulfur ions exist in the ferroelectric phase).

The TL spectrum of type I SPS crystal contains several sharp glow maxima below 100 K, which are characterized by activation energy near 0.1 eV [13, 14]. For the type
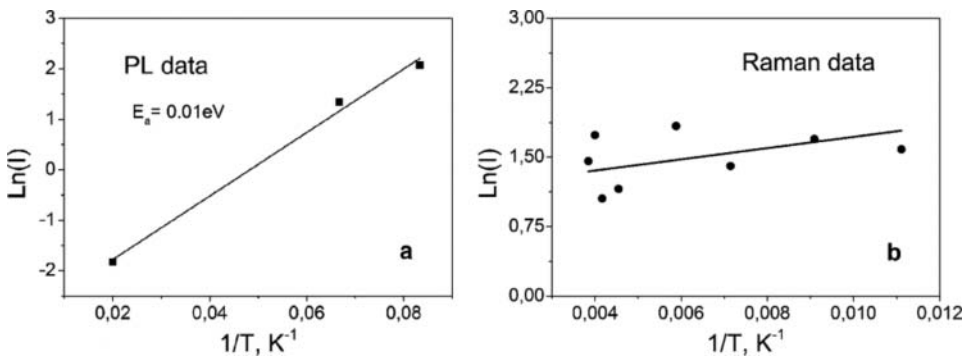
Figure 9. Semilogarithmic plots for temperature dependence of photoluminescence spectral band with number 4 for SPS sample type I (a) and for addition Raman spectral line (b).
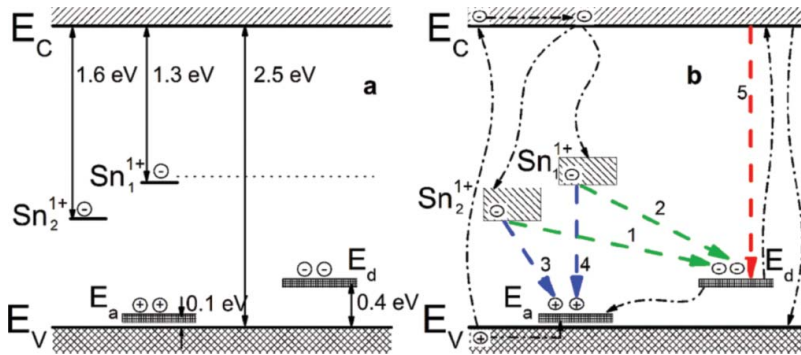
Figure 10. Energy diagram (a) for acceptor (E_a), donor (E_d) and small electronic polarons (Sn_1^{1+}, Sn_2^{1+}) energy levels in SPS crystals with vacancies of tin and sulfur [7]. At (b) the electron excitation and recombination processes are shown. The arrows with numbers from 1 till 5 show the radiation recombination processes that are related to similar number spectral bands of photoluminescence (Fig. 8).

II SPS sample the TL spectrum has several smeared glow lines below 100 K, but here additional glow lines appear – weak lines in temperature range 100–200 K with activation energy near 0.2 eV and enough strong and wide glow lines in 200–250 K temperature range with activation energy near 0.5 eV [14].
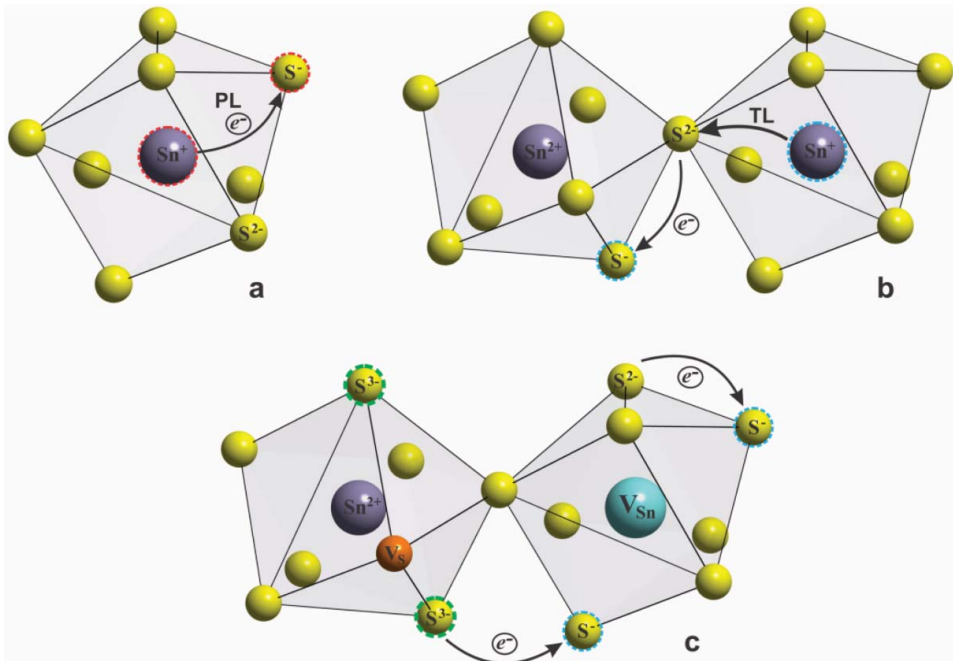
Figure 11. Schemes for hole and electron polaron annihilation at photoluminescence (a), for hole polaron hopping and further annihilation with electron polaron at thermoluminescence (b) and for hole polaron orientational (in given sulfur dodecahedron) and translational (between different sulfur dodecahedron) hopping with donor-acceptor compensation (c).

Again, the TL spectrum below 100 K for the type I sample is more intensive than this one for the type II sample. This TL obviously is related to the radiation annihilation of free electron and hole polarons, which are conserved (after excitation light removing) and could recombine after thermal hopping (Fig. 11b) till reaching of the recombination distance, what occurs at heating till 100 K. Obviously, the hole polarons have higher mobility than electron polarons, and different positions of eight sulfur ions, that build the dodecahedron surrounded by the tin cations (Fig. 11), determine several (seven) glow peaks in the TL spectrum below 100 K.

For the type II sample the TL glow lines in between 100–250 K obviously are related to the thermal hopping of bounded polarons at presence of high concentration of the sulfur vacancies with strong electric dipoles (Fig. 11c).

In general, it could be concluded that at $T < 100$ K the light excited free hole polarons S^- hopping occurs, inside of dodecahedron of sulfur ions around the tin cations, with activation energy $E_a \approx 0.1$ eV. At heating till 100 K the most intensive spectral lines "3" and "4" (near 1.5 eV and 1.7 eV) are suppressed with $E_a \approx 0.01$ eV (Fig. 9), which is determined by temperature motions (relaxations) of the order parameter (spontaneous polarization) in the three-well potential. This is illustrated by observed temperature dependence of intensity of additional line in the Raman spectrum (Fig. 7), which at heating also grow in similar activation manner (Fig. 9).

At 100–250 K range already bounded polarons recombine due to more intensive thermal motions of ions and smaller nonequivalence of chemical bonds in this temperature interval, which follows from the shape of three-well local potential (Fig. 7). At $T \geq 200$ K obviously, the donor-acceptor compensation with the activation energy $E_a \approx 0.5$ eV is involved into radiation polaronic decay processes (Fig. 11c).

So, observed activation energies are related to the shape of local potential (≈ 0.01 eV), and to the acceptors and hole polarons (≈ 0.1 eV) and donors (≈ 0.5 eV) activation energies. Now, with account of these characteristic energies we will interpret the dielectric relaxation processes. The lowest temperature relaxations (near 60 K) with $E_a \approx 0.1$ eV could be related with reorientations of hole polarons inside given dodecahedron of sulfur ions (Fig. 11c). The intermediate dielectric losses maximum (near 190 K at 10^4 Hz) is obviously related to reorientations of hole polarons that already are promoted by smaller nonequivalence of the chemical bonds and bigger amplitudes of ions thermal motions at $T \geq 100$ K. The highest temperature dielectric relaxations with losses maximum near 270 K at 10^4 Hz with $E_a \approx 0.5$ eV could be related with translational motion of the hole polarons, which is supported by the donor-acceptor compensation (Fig. 11c).

Different trends of lighting influence also could be explained in described polaronic scheme with acceptor and donor states of tin vacancies (V_{Sn}) and sulfur vacancies (V_S). For the VT sample with high concentration of acceptors (V_{Sn}), lighting increases concentration of hole polarons by excitation of electron from top of valence band into conduction band and, further, by creation of electron polarons (Fig. 10). At this, dielectric relaxations related to hole polarons are enforced. For the Br sample with high concentration of donor centers (V_S) at illumination, electrons are excited from donor level into conduction band, and after that create the electronic polarons. At this, the donor-acceptor compensation process is suppressed and dielectric relaxation anomalies become smaller.

Now it must be mentioned that dielectric relaxation are observed in dark conditions, when in fact only hole polarons are involved. These polarons are created by tin vacancies, which are presented in all SPS samples, and with especially high concentration in the VT samples. For the Br SPS samples usually high concentration of sulfur vacancies is presented that induce the donor states with strong electric dipoles. Such polar defects could

determine addition bounding of hole polarons in SPS crystal lattice. Of course, different concentrations of intrinsic and extrinsic defects could determine wide set of trapping centers for the charge carriers in SPS crystals. By this, the specter of relaxation times for the hole polarons dielectric contribution could be different.

As mentioned earlier [8], for SPS crystals with high concentration of tin vacancies, and hole polarons, big electric conductivity is observed and strong rise of dielectric losses in the paraelectric phase at high temperatures is reached (Fig. 2). For SPS crystals with big concentration of sulfur vacancies the electric conductivity is low, which corresponds to smaller concentration of acceptor centers, and their effective compensation. Moreover the strong bounding of polarons by strong electric dipoles of sulfur vacancies determines their low mobility and low dielectric losses at heating in the paraelectric phase (Fig. 1).

Strong pinning of the domain walls in the ferroelectric phase, just below T_0, is determined by charge carriers in VT SPS samples with high conductivity. Weak pinning of the domain walls by local dipole defects is realized in Br SPS samples with low electric conductivity. Obviously, in latter case conditions for the temperature hysteresis of the domain walls dielectric contribution are presented.

IV. Conclusions

For $Sn_2P_2S_6$ semiconductor crystals with local three-well potential in ground state, that is related to the chemical bonds change and charge transfer at transition into the ferroelectric phase, the low frequency dielectric susceptibility relaxation anomalies and their variation under illumination could be related to the small hole polarons dynamics with donor-acceptor compensation processes in lattice with tin and sulfur vacancies. Both the temperature dependence of Raman spectral bands shape, which characterizes the crystal lattice anharmonicity, and observed [12, 13] photoluminescence temperature suppression coincide with the energy barrier in local potential. The activation energies for the dielectric relaxation processes and for thermoluminescence glow spectral bands [14] correlate with in gap energy positions of tin vacancies shallow acceptor states and sulfur vacancies dip donor states and give evidence about polarons dynamics at involving in donor-acceptor compensation.

References

1. A. A. Grabar, Yu. M. Vysochanskii, A. N. Shumelyuk, M. Jazbinsek, G. Montemezzani, and P. Gunter, *Photorefractive effect in the red and near infra red regions of spectrum*. In: P. Gunter, J. Huignard, eds. *Photorefractive materials and their applications*. (Springer Verlag, Heidelberg 2006).
2. S. K. Choi, B. S. Kang, Y. W. Cho, and Yu. M. Vysochanskii, Diffuse dielectric anomaly in ferroelectric materials. *J. Electroceram.* **13**, 493–502 (2004).
3. M. M. Maior, M. I. Gurzan, S. B. Molnar, I. P. Prits, and Yu. M. Vysochanskii, Effect of germanium doping on pyroelectric and piezoelectric properties of $Sn_2P_2S_6$ single crystal. *IEEE Trans. Ultrason. Ferroelectr. Freq. Control* **47**, 877–880 (2000)
4. Yu. M. Vysochanskii, T. Janssen, R. Currat, R. Folk, J. Banys, J. Grigas, and V. Samulionis, *Phase transitions in ferroelectric phosphorous chalkogenide crystals*. (Vilnius University Publishung House, Vilnius 2006).
5. K. Rushchanskii, Yu. Vysochanskii, and D. Strauch, Ferroelectricity, nonlinear dynamics and relaxation effects in monoclinic $Sn_2P_2S_6$. *Phys. Rev. Lett.* **99**, 207601 (2007).
6. K. Glukhov, K. Fedyo, and Yu. Vysochanskii, Electronic structure and phase transition in ferroelectric $Sn_2P_2S_6$ crystal. arXiv:1108.2390v2 [cond-mat.mtrl-sci].

7. Yu. Vysochanskii, K. Glukhov, K. Fedyo, and R. Yevych, Charge transfer and anharmonicity in Sn$_2$P$_2$S$_6$ ferroelectrics. *Ferroelectrics* **414**, 30–40 (2011).

8. Yu. Vysochanskii, K. Glukhov, M. Maior, K. Fedyo, A. Kohutych, V. Betsa, I. Prits, and M. Gurzan, Ferroelectric and semiconducting properties of Sn$_2$P$_2$S$_6$ crystals with intrinsic vacancies. *Ferroelectrics* **418**, 124–133 (2011).

9. A. Rudiger, Light induced charge transfer processes and pyroelectric luminescence in Sn$_2$P$_2$S$_6$, Ph D Thesis, Osnabruk: University of Osnabruk (2001).

10. A. Rudiger, O. Schirmer, S. Odoulov, A. Shumelyuk, and A. Grabar, Studies of light-induced charge transfer in Sn$_2$P$_2$S$_6$ by combined EPR/optical spectroscopy. *Opt. Mater.* **18**, 123–125 (2001).

11. O. Bidault, M. Maglione, M. Actis, M. Kchikech, and B. Salke, Polaronic relaxation in perovskites. *Phys. Rev. B* **52**, 4191–4197 (1995).

12. Z. Potucek and Z. Bryknar, Photoluminescence of defects in Sn$_2$P$_2$S$_6$. *Ferroelectrics* **334**, 171–179 (2006).

13. Z. Potucek, Z. Bryknar, and P. Ptacek, Luminescence spectroscopy of Sn$_2$P$_2$S$_6$ crystals. *Ferroelectrics* **304**, 181–185 (2004).

14. Z. Potucek, P. Ptacek, and Z. Bryknar, Thermoluminescence of Sn$_2$P$_2$S$_6$ crystals. *Phys. Status Solidi C* **2**, 560–563 (2005).

15. M. Iwata, A. Miyashita, Y. Ishibashi, K. Moriya, and S. Yano, Low temperature dielectric dispersion in Sn$_2$P$_2$S$_6$. *J. Phys. Soc. Jpn.* **67**, 499–501 (1998).

16. M. Maior, S. Molnar, V. Vrabel, M. Gurzan, S. Motrja, and Yu. Vysochanskii, Dielectric relaxation and freezing effect in Sn$_2$P$_2$S$_6$. *Condens. Matter Phys.* **6**, 293–299 (2003).

17. K. Oshiba and T. Hotta, Strong-coupling theory of rattling-induced superconductivity. *J. Phys. Soc. Jpn.* **80**, 094712–094718 (2011).